^{99m}Tc-Labeled Interleukin 8 for the Scintigraphic Detection of Infection and Inflammation: First Clinical Evaluation

Chantal P. Bleeker-Rovers[1,2,3], Huub J.J.M. Rennen[1], Otto C. Boerman[1], Ate B. Wymenga[4], Eric P. Visser[1], Johannes H. Bakker[5], Jos W.M. van der Meer[2,3], Frans H.M. Corstens[1,2], and Wim J.G. Oyen[1,2]

[1]Department of Nuclear Medicine, Radboud University Nijmegen Medical Centre, Nijmegen, The Netherlands; [2]Centre for Infectious Diseases, Nijmegen University, Nijmegen, The Netherlands; [3]Department of Internal Medicine, Radboud University Nijmegen Medical Centre, Nijmegen, The Netherlands; [4]Department of Orthopedic Surgery, Sint Maartenskliniek, Nijmegen, The Netherlands; and [5]Department of Clinical Pharmacy, Radboud University Nijmegen Medical Centre, Nijmegen, The Netherlands

Interleukin 8 (IL-8) is a chemotactic cytokine that binds with a high affinity to receptors expressed on neutrophils. Previous studies with various animal models showed that ^{99m}Tc-labeled IL-8 accumulates specifically and rapidly in infectious and inflammatory foci. The aims of the present study were to evaluate the safety of IL-8 in humans and to assess the value of ^{99m}Tc-IL-8 scintigraphy in patients with suspected localized infections. **Methods:** ^{99m}Tc-IL-8 was intravenously injected at 400 MBq into 20 patients with various suspected localized infections. Patients were monitored for IL-8–related side effects for 4 h. Whole-body imaging was performed directly after injection and at 4 h after injection. Imaging after 24 h was performed for the first 7 patients and for subsequent patients when the results of ^{99m}Tc-IL-8 scintigraphy at 4 h after injection were normal or equivocal. Blood was drawn at several time points to determine the total number of leukocytes and leukocyte differentiation (all patients) and to determine pharmacokinetics (6 patients). **Results:** ^{99m}Tc-IL-8 scintigraphy was performed for 20 patients (13 men and 7 women) with a mean age of 60 y (range, 21–76 y). No significant side effects were noted. Patients had suspected joint prosthesis infections ($n = 9$), osteomyelitis ($n = 8$), liver abscess ($n = 1$), and soft-tissue infections ($n = 2$). ^{99m}Tc-IL-8 was rapidly cleared from the blood and most other organs. In 10 of 12 patients with infections, ^{99m}Tc-IL-8 localized the infection at 4 h after injection. In 1 patient with vertebral osteomyelitis and in 1 patient with an infected knee prosthesis, ^{99m}Tc-IL-8 scintigraphy results were false-negative. In 8 patients with noninfectious disorders, no focal accumulation of ^{99m}Tc-IL-8 was found. **Conclusion:** Injection of ^{99m}Tc-IL-8 is well tolerated. ^{99m}Tc-IL-8 scintigraphy is a promising new tool for the detection of infections in patients as early as 4 h after injection.

Key Words: interleukin 8; infection; imaging; ^{99m}Tc

J Nucl Med 2007; 48:337–343

To enable the adequate management of patients with infectious and inflammatory diseases, timely identification of the localization and the extent of infectious and inflammatory foci is crucial. The value of labeled leukocyte scintigraphy for the imaging of infection and inflammation is well documented, but the labeling procedure is laborious and time-consuming and requires the handling of potentially infected blood products. Furthermore, the optimal imaging time, especially for labeling with ^{111}In, can be as long as 24 h after injection. A rapid, in vivo method for labeling leukocytes would overcome many of these limitations and is highly desirable.

Interleukin 8 (IL-8), a small protein (8.5 kDa) that belongs to the CXC subfamily of chemokines, which play an important role in cell recruitment during acute inflammation (*1*), is an interesting candidate for the in vivo labeling of neutrophils. Neutrophils abundantly express 2 types of IL-8 receptors (CXC1 and CXC2) (*2,3*) to which IL-8 binds with a high affinity (*4,5*). A ^{99m}Tc-labeled IL-8 preparation was developed with hydrazinonicotinamide (HYNIC) as a chelating agent (*6*). This preparation showed promising characteristics for the imaging of infection and inflammation in various experimental models, including intramuscular infections (*6,7*), colitis (*8*), osteomyelitis (*9*), and various pulmonary infections (*10*). Neutrophil-driven specificity was demonstrated by a 90% reduction in the uptake of ^{99m}Tc-IL-8 in abscesses in neutropenic rabbits compared with abscess uptake in normal rabbits (*7*).

The side effects of IL-8 appear to be limited. The administration of IL-8 at 10–100 μg/kg to nonhuman primates and rabbits resulted in a temporary decrease in the number of circulating granulocytes, which normalized after 5–30 min, and then an increase in the number of circulating granulocytes, which reached a maximum after 120 min (*11,12*). Intravenous injection of IL-8 at 40 ng/kg–1 μg/kg into rabbits or baboons resulted in only a temporary decrease in the number of circulating granulocytes,

without subsequent granulocytosis (11,13). In rabbits, this effect was shown to be dose related, and the administration of IL-8 at 2 ng/kg did not have any effect on the number of granulocytes (11). The administration of ^{131}I-IL-8 at 50–100 μg to 11 patients with soft-tissue infections resulted in a brief decrease in the number of leukocytes (mean, 0.6×10^9/L), with complete normalization after 1 h (14). The encouraging results of our experimental studies and the apparent safety of a low dose of IL-8 led to the present study, in which we evaluated the safety of IL-8 in humans and assessed the value of [99mTc]-IL-8 scintigraphy in patients with suspected localized infections.

MATERIALS AND METHODS

Patients

Patients who were 18 y or older and who had suspected localized infections were recruited by infectious diseases specialists or orthopedic surgeons specializing in treating patients with bone or joint infections at Radboud University Nijmegen Medical Centre, and at Sint Maartenskliniek, Nijmegen, The Netherlands. Pregnant or lactating patients, patients with a creatinine clearance of less than 50 mL/min, patients diagnosed with myocardial infarction in the previous 6 mo, and patients with significant electrocardiographic changes (ischemia, left bundle branch block, or second- or third-degree atrioventricular block) were excluded. The study was approved by local ethics committees, and written informed consent was obtained from all patients.

For all patients, measurements of hemoglobin, leukocyte counts, differentiation of leukocytes, platelet counts, electrolytes, creatinine, alkaline phosphatase, alanine aminotransferase, and lactate dehydrogenase were obtained directly before and at 1 h after the injection of IL-8. For the first 7 patients, these parameters were also measured at 24 h after injection, and electrocardiography was performed directly before and at 24 h after IL-8 injection. In addition, for these patients, blood samples for the determination of the number and differentiation of leukocytes and for measurement of the blood clearance of [99mTc]-IL-8 were obtained at −1, 1, 5, 10, 15, 30, 60, 120, and 240 min after the injection of IL-8. Vital signs were recorded up to 2 h after injection. The final diagnosis was established by the attending physician and the first author, who was not involved in reading of the [99mTc]-IL-8 images. A definite diagnosis was based on positive culture results, histology, or surgery. When a definite diagnosis was not possible, a probable diagnosis was made on the basis of a combination of clinical follow-up of at least 3 mo, response to specific therapy, and conventional imaging studies. The final diagnosis served as a standard of reference and was used for comparison with the results of [99mTc]-IL-8 scintigraphy.

Conjugation of HYNIC to IL-8

Synthetic human IL-8 was synthesized under conditions of good manufacturing practice by RMF Dictagene SA. Lyophilized samples of 250 μg were stored at 4°C. N-(Tris(hydroxymethyl)-methyl)glycine (Tricine) was purchased from Fluka. Glycine, nicotinic acid, polyoxyethylenesorbitan monooleate (Tween 80), and 2-(N-morpholino)ethanesulfonic acid (MES) were purchased from Sigma-Aldrich. The propylaldehyde hydrazone of succinimidyl-hydrazinonicotinic acid was synthesized essentially as described previously (15,16). The IL-8–HYNIC conjugate was prepared as described previously (17), with some minor modifications. In brief, a sample of 250 μg of synthetic human IL-8 was reconstituted in 45 μL of buffer (50 mM MES [pH 6.5] and 0.32 M NaCl), and 5 μL of 1 M NaHCO₃ (pH 8.2) was added. Subsequently, a 3-fold molar excess of HYNIC in 5 μL of dry dimethyl sulfoxide was added dropwise to the mixture. After incubation for 10 min at room temperature, the reaction was stopped by the addition of an excess of glycine (50 μL; 1.0 M glycine in phosphate-buffered saline [PBS]). Next, 0.9 mL of PBS was added, and the mixture was extensively dialyzed against PBS (0.5- to 3.0-mL dialysis cell with a molecular weight cutoff of 3,500; Pierce) to remove excess unbound HYNIC. After dialysis, a polyoxyethylenesorbitan monooleate solution (0.1% in PBS) was added to the IL-8–HYNIC conjugate to a total volume of 10 mL to reduce sticking of the protein to the vial. Samples of 10 μg of IL-8–HYNIC in 400 μL of polyoxyethylenesorbitan monooleate solution (0.1% in PBS) were stored at −20°C.

Radiolabeling Procedure

A lyophilized coligand kit was prepared to contain 30 μg of SnSO₄, 45 mg of N-(tris(hydroxymethyl)-methyl)glycine, and 4 mg of nicotinic acid. The coligand kit was reconstituted with 600 μL of a 0.9% NaCl solution immediately before the start of the radiolabeling procedure. To a 10-μg IL-8–HYNIC sample, 400 μL of a reconstituted coligand kit was added, together with 800–1,000 MBq of [99mTc]O₄⁻ in saline. The mixture was incubated at 70°C for 30 min. The radiochemical purity was determined by instant thin-layer chromatography on ITLC-SG strips (Gelman Laboratories) with 0.1 M citrate (pH 6.0) as the mobile phase. After the labeling reaction was complete, the reaction mixture was diluted with a 0.9% NaCl solution to a final concentration of 40 MBq/mL. The preparation was approved for use in patients when the radiochemical purity exceeded 90%. A 10-mL quantity of the final preparation was intravenously administered to a patient over 5 min by use of an infuser (Asena; Alaris Medical Systems).

Image Acquisition and Analysis

Scintigraphic images were obtained with a dual-head γ-camera (ECAM; Siemens) equipped with low-energy, high-resolution, parallel-hole collimators (140-keV photopeak, 15% symmetric window). All images were collected in a $256 \times 1,024$ matrix. Whole-body scans were recorded directly after injection (scan speed, 10 cm/min) and after 4 h (scan speed, 5 cm/min) for all patients. For the first 7 patients, whole-body scans were also obtained after 24 h (scan speed, 4 cm/min); for the remaining patients, whole-body scans were obtained after 24 h only when the results of scans obtained after 4 h were normal or equivocal. When indicated, static images in a 256×256 matrix were acquired at 4 and 24 h after injection for preset times of 5 and 10 min, respectively. Images were read by 2 nuclear medicine physicians who were unaware of the results of verification procedures. The results of [99mTc]-IL-8 scans were regarded as positive when focal accumulation of the tracer was observed.

Dosimetry

To estimate the radiation-absorbed doses for the patients, dosimetric analysis of the whole-body scintigraphic images was performed for 13 men and 7 women by use of the conjugate view technique with partial background subtraction and correction for attenuation as described previously (18,19). Briefly, regions of interest (ROIs) over the whole body and organs of interest (liver, spleen, kidneys, and skull) were drawn on the posterior or anterior

scintigraphic images. The skull ROIs were used to calculate the red bone marrow dose residence time, with the assumption that a fixed fraction of the total red bone marrow content was present in the skull (20). Organ radioactivity as the percentage injected dose (%ID) was estimated by designating the whole-body ROI of the first scan as 100% of the administered dose, corrected for the physical decay between the injection time and the first scan. Subsequently, the residence times of activity in organs of interest were calculated by use of trapezoid integration. The whole-body biologic half-life ($t_{1/2}$), to be used in the dynamic bladder model, was calculated by use of a monoexponential fit. Radiation-absorbed doses for organs were calculated by use of the OLINDA program (21) with the adult male phantom for men, the adult female phantom for women, and the dynamic bladder model (fraction 1; bladder voiding at 4 h).

RESULTS

^{99m}Tc-IL-8 scintigraphy was performed for 20 patients (13 men and 7 women) with a mean age of 60 y (range, 21–76 y) and with suspected focal infections (Table 1). Patients had suspected joint prosthesis infections ($n = 9$), osteomyelitis ($n = 8$), liver abscess ($n = 1$), and soft-tissue infections ($n = 2$). The median duration of symptoms before ^{99m}Tc-IL-8 scintigraphy was performed was 6 mo (range, 1 wk–48 mo). In the patients with suspected joint prosthesis infections, the median duration between insertion of the prosthesis and ^{99m}Tc-IL-8 scintigraphy was 22 mo (range, 6–192

mo). Various infections were diagnosed in 12 patients: 5 cases of osteomyelitis, 5 joint prosthesis infections, 1 soft-tissue infection, and 1 liver abscess. All infections were confirmed by culturing, histology, or surgery.

Scintigraphy with ^{99m}Tc-IL-8 correctly identified the infection in 10 patients (Figs. 1–3). In all of these patients, the infection was clearly delineated at 4 h after injection. In most patients, visualization of the infection did not improve further after 24 h, except for the patient with the liver abscess, in whom the infection was more clearly visualized at 24 h after injection (Fig. 1). In patient 4, who was diagnosed with vertebral osteomyelitis, and patient 17, who had a chronic low-grade infection of her knee prosthesis, the results of ^{99m}Tc-IL-8 scintigraphy were considered false-negative. Patient 4 had been treated with antibiotics for cholangitis with *Escherichia coli* bacteremia 3 mo before he was readmitted with back pain and fever. Vertebral osteomyelitis of L2 and L3 was diagnosed after bone scintigraphy and MRI. This diagnosis was confirmed by percutaneous biopsy of the vertebra; the culture of the specimen also yielded *E. coli*. The ^{99m}Tc-IL-8 scintigraphy results were considered normal. Patient 17 had complained of knee pain since insertion of her knee prosthesis 18 mo before ^{99m}Tc-IL-8 scintigraphy. Her temperature was normal and, except for a painful knee, she did not have any symptoms or signs; therefore, clinically, the suggestion of

TABLE 1
Clinical Characteristics, Results of ^{99m}Tc-IL-8 Scintigraphy, Verification Procedures, and Final Diagnoses for 20 Patients with Various Suspected Infectious Foci

Patient (sex/age [y])	Suspected focus	^{99m}Tc-IL-8 scintigraphy results	Verification	Final diagnosis	Follow-up (mo)
1 (F/53)	Pelvic abscess with fistula	+ (TP)	C (*Pseudomonas aeruginosa*)	Pelvic abscess with fistula	3
2 (M/61)	Caval filter	− (TN)	R, FU	Caval filter not infected	18
3 (M/76)	Knee prosthesis	+ (TP)	S, H (chronic inflammation and osteomyelitis	Infected knee prosthesis	12
4 (M/66)	Vertebral osteomyelitis	− (FN)	S, C (*Escherichia coli*)	Vertebral osteomyelitis	3
5 (M/31)	Humerus	+ (TP)	C (*Staphylococcus epidermidis*)	Osteomyelitis of shoulder	11
6 (M/74)	Ankle	− (TN)	H (leukocytoclastic vasculitis), FU	Vasculitis, no infection	6
7 (M/21)	Liver	+ (TP)	C (*Staphylococcus aureus*), S	Liver abscess	6
8 (M/76)	Total hip prosthesis	+ (TP)	S, C (*Streptococcus bovis*)	Infected total hip prosthesis	3
9 (M/42)	Calcaneus	+ (TP)	C (streptococci, *S. epidermidis*)	Osteomyelitis of calcaneus	4
10 (F/64)	Calcaneus	+ (TP)	S, H (chronic osteomyelitis)	Osteomyelitis of calcaneus	4
11 (M/53)	Ankle	+ (TP)	S	Osteomyelitis of ankle	4
12 (M/63)	Total hip prosthesis	− (TN)	R, FU	Spinal stenosis, no infection	5
13 (F/76)	Total hip prosthesis	+ (TP)	S	Infected total hip prosthesis	4
14 (M/76)	Elbow prosthesis	+ (TP)	S	Infected elbow prosthesis	4
15 (M/63)	Knee prosthesis	− (TN)	R, FU	Aseptic loosening	8
16 (F/67)	Knee	− (TN)	R, FU	Osteoarthritis	9
17 (F/72)	Knee prosthesis	±* (FN)	S, C	Infected knee prosthesis	9
18 (F/65)	Knee prosthesis	− (TN)	R, FU	Arthrofibrosis	4
19 (M/44)	Knee	− (TN)	S, C, FU	Osteoarthritis	6
20 (F/58)	Total hip prosthesis	− (TN)	S, C, FU	Aseptic loosening	5

*± = results were considered equivocal; slightly increased uptake of ^{99m}Tc-IL-8 was seen at medial side of tibia.
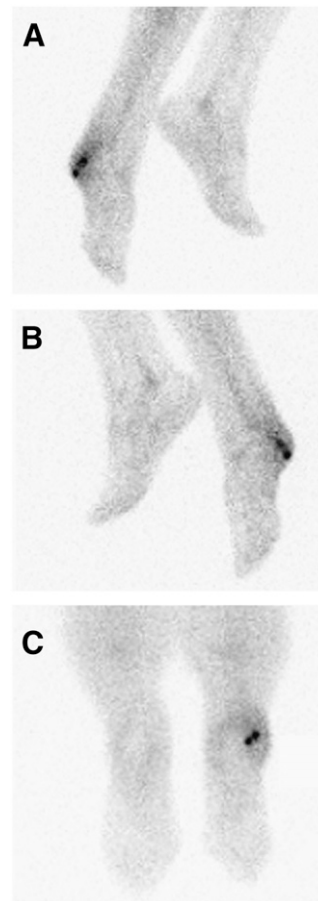
TP = true-positive; C = culturing; TN = false-negative; R = radiology; FU = clinical follow-up of at least 3 mo without antibiotic treatment; S = surgery; H = histology; FN = false-negative.
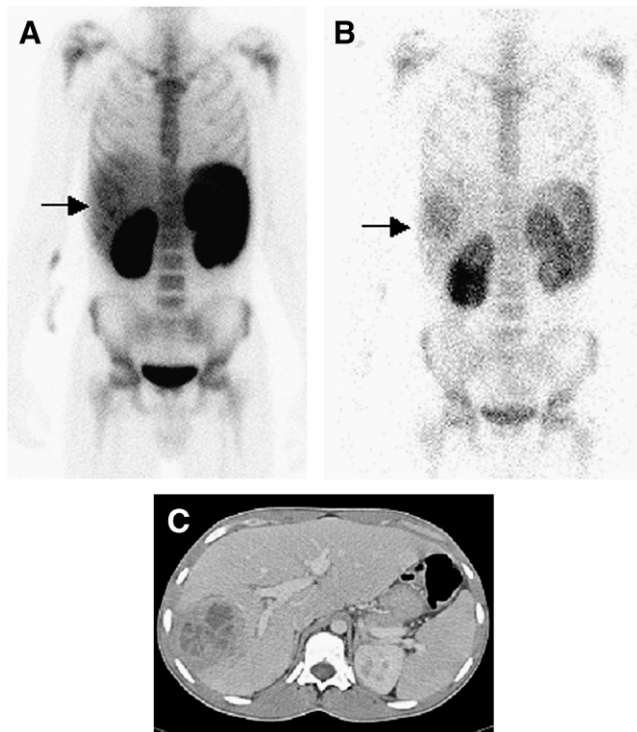
FIGURE 1. This 21-y-old man (patient 7) had medical history of chronic granulomatous disease and relapsing liver abscesses. He was admitted with fever and abdominal discomfort. (A) At 4 h after injection of ^{99m}Tc-IL-8, scintigraphy showed focal accumulation of tracer in liver (arrow). (B) Infection was more clearly visualized after 24 h (arrow). (C) Abdominal CT confirmed the presence of a large liver abscess.


FIGURE 2. This 64-y-old woman (patient 10) had traumatic deformation of the right foot followed by several episodes of osteomyelitis between 1944 and 1965. For 6 mo she had experienced pain, redness, and swelling of the right foot. ^{99m}Tc-IL-8 scintigraphy at 4 h after injection showed increased uptake in the calcaneus of the right foot (A: lateral right and medial left; B: medial right and lateral left; C: plantar). A fistula draining pus developed, which was treated with antibiotics. One week later, surgical debridement revealed clear signs of infection; therefore, osteomyelitis was diagnosed. Culture results were negative, but histologic samples confirmed the diagnosis of chronic osteomyelitis.

infection was low. The results of ^{99m}Tc-IL-8 scintigraphy were considered equivocal; slightly increased uptake of ^{99m}Tc-IL-8 was seen at the medial side of the tibia. Because of continuing complaints of pain, revision of the knee prosthesis was scheduled 7 mo later. Cultures of deep specimens of the medial side of the tibia obtained at this time yielded *Propionibacterium acnes,* whereas the results of cultures of specimens from the femoral component and the lateral side of the tibia were negative. Histology showed chronic inflammation, and the final diagnosis was an infected knee prosthesis.

The remaining 8 patients were diagnosed with various noninfectious disorders on the basis of radiology and clinical follow-up of at least 3 mo (median, 6 mo; range, 4–18 mo). In 3 of these patients, infection was definitely excluded by culturing, histology, or surgery (patients 6, 19, and 20). For all 8 patients, the results of ^{99m}Tc-IL-8 scintigraphy were normal, so that for the total group of 20 patients, ^{99m}Tc-IL-8 scintigraphy results were true-positive for 10 patients, true-negative for 8 patients, and false-negative for 2 patients. For these 20 patients, the sensitivity of ^{99m}Tc-IL-8 scintigraphy was 83%, the specificity was 100%, and the accuracy was 90%. Three patients also had a malignancy at the time of ^{99m}Tc-IL-8 scintigraphy; patient 1 had a squamous cell carcinoma of the bladder, patient 6

had prostate cancer with bone metastases, and patient 8 had recently been diagnosed with colon carcinoma with lung metastases. ^{99m}Tc-IL-8 uptake was not observed in any of the patients with tumors. In addition to ^{99m}Tc-IL-8 scintigraphy, IgG scintigraphy was performed for patients 3 and 5. For both of these patients, the results of IgG scintigraphy were normal, whereas ^{99m}Tc-IL-8 scintigraphy visualized the infection, which was confirmed by histology or culturing. For patient 1, ^{18}F-FDG PET was performed a few days before ^{99m}Tc-IL-8 scintigraphy. Compared with an ^{18}F-FDG PET scan obtained 6 mo earlier, this PET scan showed unchanged ^{18}F-FDG uptake in the pelvic tumor and multiple fistulas, but a new fistula from the pelvic tumor to the medial side of the right leg was found; this finding corresponded to the uptake of IL-8. Infection of this fistula was confirmed by positive culture results.

Patient 1, with a history of hyperventilation, experienced mild flushing of the face within 5 min after the bolus injection; this effect subsided spontaneously within 15 min. None of the other patients experienced any side effects within 5 min after the injection of IL-8, nor were there any significant changes in hematologic or biochemical values.

Figure 1 shows representative whole-body images at 4 and 24 h after the injection of ^{99m}Tc-IL-8. These images clearly demonstrate the physiologic uptake of ^{99m}Tc-IL-8 in the kidneys, bone marrow, liver, and spleen. The
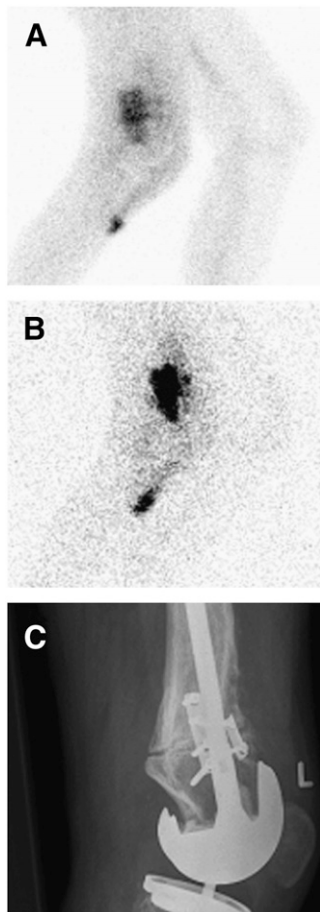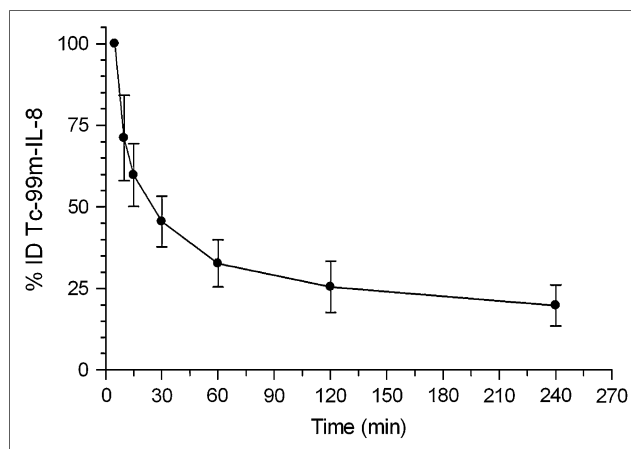
FIGURE 3. This 76-y-old man (patient 3) developed a fistula draining pus below his knee 1 mo after he received a total knee prosthesis. ^{111}In-IgG scintigraphy showed increased uptake in the fistula, but not anywhere near the knee prosthesis. Clinical suggestion of infection remained high. (A and B) ^{99m}Tc-IL-8 scintigraphy showed increased uptake in the fistula as well as at the femoral end of the prosthesis (A: 4 h after injection; B: 24 h after injection). During surgery, a large abscess surrounding the femoral component of the prosthesis was drained. (C) Radiograph of the total knee prosthesis.

FIGURE 4. Blood clearance of ^{99m}Tc-IL-8 in patients with suspected focal infections. Data are expressed as %ID in blood pool. Error bars indicate SEMs.

biodistribution of ^{99m}Tc-IL-8 changed little over a 24-h imaging interval. The uptake in the larger blood vessels, heart, lungs, and gastrointestinal tract was low. Analysis of the blood clearance showed a $t_{1/2\alpha}$ of 7.5 $\pm$ 0.9 min and a $t_{1/2\beta}$ of 4.6 $\pm$ 0.8 h (Fig. 4). The mean whole-body retention values at 4 and 24 h after injection were 86 $\pm$ 5 %ID and 71 $\pm$ 6 %ID, respectively. The estimated mean radiation-absorbed doses of ^{99m}Tc-IL-8 in the total body and organs are shown in Table 2. In line with the high and persistent uptake in the kidneys on the images, the kidneys showed the highest absorbed dose, approximately 100 μGy/MBq. The administration of a typical dose of 400 MBq of ^{99m}Tc-IL-8 will result in an effective dose of 2.7 mSv.

DISCUSSION

In this report, the first clinical results of ^{99m}Tc-IL-8 scintigraphy for patients with suspected infections are described. In several experimental models (6–10), ^{99m}Tc-IL-8 has shown many favorable characteristics, such as rapid accumulation in target tissue and rapid clearance from blood and nontarget tissues. The activity is mainly cleared through the kidneys; this clearance is an advantage over hepatobiliary clearance, because high activity in the liver and especially in the bowel would have made ^{99m}Tc-IL-8 less suitable for the imaging of infectious foci in the abdomen. In 10 of 12 patients eventually diagnosed with various, mostly orthopedic, infections, ^{99m}Tc-IL-8 rapidly accumulated in the infectious foci and clearly depicted the infection at 4 h after injection. In 1 patient with vertebral osteomyelitis, no accumulation of ^{99m}Tc-IL-8 was found. Radiolabeled leukocyte scintigraphy is known for its limited sensitivity in patients with vertebral osteomyelitis, most probably because of the relatively high uptake of radiolabeled leukocytes in normal bone marrow (22), and for minimal leukocyte infiltration in cases of vertebral osteomyelitis; these properties could also explain the false-negative results of ^{99m}Tc-IL-8 imaging in our patient with vertebral osteomyelitis. Because of the long time span between equivocal ^{99m}Tc-IL-8 scintigraphy and surgery in the patient eventually diagnosed with a chronic low-grade infection of a knee prosthesis (patient 17), the possibility that the infection originated after ^{99m}Tc-IL-8 scintigraphy cannot be excluded. It is more likely, however, that the infection was already present at the time of ^{99m}Tc-IL-8 scintigraphy and therefore that the results of ^{99m}Tc-IL-8 scintigraphy were false-negative or that the results, which were defined as being equivocal, should have been scored as positive for infection. Although the number of granulocytes decreases in chronic inflammatory infiltrates, granulocytes do not disappear, and ^{99m}Tc-IL-8 scintigraphy clearly visualized the infection in patients with symptoms existing for up to 48 mo. Further studies will be needed to determine whether comparable equivocal results should be regarded as a positive indication for infection in the future.

There was no focal accumulation of ^{99m}Tc-IL-8 in patients eventually diagnosed with various noninfectious disorders, especially not in joint prostheses showing aseptic loosening. Because aseptic loosening is the most important alternative diagnosis in most patients with suspected joint prosthesis infections and should be treated in an entirely different manner, this is a very important characteristic. Specificity is further suggested by the absence of ^{99m}Tc-IL-8 accumulation in 3 different malignant disorders. To

TABLE 2
Absorbed Doses of ^{99m}Tc-IL-8 in Organs

Organ	Absorbed dose (μGy/MBq)*	
	Mean ± SD	Range
Adrenal glands	9.6 ± 1.6	7.9–13.0
Brain	1.9 ± 0.3	1.5–2.6
Breasts	1.9 ± 0.2	1.6–2.4
Gallbladder wall	7.4 ± 0.6	6.7–8.6
LLI wall	4.2 ± 0.5	3.7–5.2
Small intestine	5.1 ± 0.4	4.5–5.7
Stomach wall	5.6 ± 0.5	4.7–6.4
ULI wall	5.0 ± 0.4	4.5–5.7
Heart wall	3.8 ± 0.3	3.3–4.5
Kidneys	96.9 ± 24.7	70.3–140.5
Liver	10.2 ± 1.0	9.2–11.9
Lungs	3.4 ± 0.3	2.9–4.2
Muscle	3.2 ± 0.2	2.9–3.8
Ovaries	5.0 ± 0.3	4.7–5.4
Pancreas	8.9 ± 0.9	7.3–10.3
Red marrow	5.4 ± 0.7	4.4–6.3
Osteogenic cells	8.7 ± 1.0	7.6–11.1
Skin	1.8 ± 0.2	1.6–2.2
Spleen	37.8 ± 15.0	19.3–65.9
Testes	2.4 ± 0.2	2.2–2.7
Thymus	2.5 ± 0.4	1.6–2.9
Thyroid	2.2 ± 0.3	1.6–2.7
Urinary bladder wall	21.9 ± 9.4	12.4–38.8
Uterus	6.2 ± 0.2	5.9–6.4
Total body	4.1 ± 0.3	3.6–4.6

*Mean ± SD (range) effective dose was 6.7 ± 1.2 (5.5–9.2) mSv/MBq.
LLI = lower large intestine; ULI = upper large intestine.

enable more exact calculations of sensitivity and specificity, new studies with larger numbers of patients are needed.

The properties of IL-8 for infection imaging in humans have been investigated in only 1 previous study with ^{131}I-IL-8 in 11 patients (14). Within 3 h, ^{131}I-IL-8 accumulated at the sites of infection in 8 patients with active diabetic foot infections and in 1 patient with cellulitis of the thumb. No uptake of ^{131}I-IL-8 was seen at the sites of successfully treated osteomyelitis in 2 patients. The results of that study can, of course, not be compared directly with the results of the present study because of the different radiolabels and different preparations of IL-8. The physical properties of ^{131}I, for example, limit the spatial resolution and the delineation of small structures. Moreover, in rabbits with *E. coli* infection, oxidative iodination has been shown to result in deterioration of the imaging characteristics of IL-8 (6,23).

^{99m}Tc-IL-8 cleared rapidly from nontarget tissues, except for the liver, spleen, and bone marrow. In all patients, the infection was visualized at 4 h after injection. In most patients, visualization of the infection did not improve significantly after 24 h, except for the patient with the liver abscess. In this case, the infection was more clearly visualized at 24 h after injection because of decreasing background activity.

There were no significant side effects after the injection of ^{99m}Tc-IL-8. Peripheral leukocyte counts did not change significantly, most probably because of the low dose of IL-8. Patients received between 5 and 10 μg of IL-8, corresponding to a dose of less than 100 ng/kg; this dose is 10 times lower than the dose of 1 μg/kg used in the study of Gross et al. (14), which resulted in a transient reduction in the leukocyte count (mean, 4%; range, 3%–14%) in 6 of 11 patients. The transient flushing of the face directly after a bolus injection of ^{99m}Tc-IL-8 cannot readily be explained by the physiologic effects of IL-8. It is unclear whether this reaction was actually caused by the administration of IL-8, because it was not encountered in the remaining 19 patients.

CONCLUSION

This first clinical evaluation of ^{99m}Tc-IL-8 scintigraphy demonstrated that injection of ^{99m}Tc-IL-8 is well tolerated and allows the detection of various infections in patients at 4 h after injection. Because of its favorable characteristics, such as obviating the need for the handling of infected blood products, rapid accumulation at the site of infection, rapid clearance from the blood pool and nontarget tissues, and absence of significant side effects, ^{99m}Tc-IL-8 scintigraphy is a promising infection imaging technique. For further evaluation of the clinical value of ^{99m}Tc-IL-8 scintigraphy, clinical studies with larger numbers of patients with various infectious or noninfectious inflammatory diseases are warranted.

REFERENCES

1. Ben-Baruch A, Michiel DF, Oppenheim JJ. Signals and receptors involved in recruitment of inflammatory cells. *J Biol Chem.* 1995;270:11703–11706.
2. Holmes WE, Lee J, Kuang WJ, Rice GC, Wood WI. Structure and functional expression of a human interleukin-8 receptor. *Science.* 1991;253:1278–1280.
3. Murphy PM, Tiffany HL. Cloning of complementary DNA encoding a functional human interleukin-8 receptor. *Science.* 1991;253:1280–1283.
4. Lee J, Horuk R, Rice GC, Bennett GL, Camerato T, Wood WI. Characterization of two high affinity human interleukin-8 receptors. *J Biol Chem.* 1992;267: 16283–16287.
5. Patel L, Charlton SJ, Chambers JK, Macphee CH. Expression and functional analysis of chemokine receptors in human peripheral blood leukocyte populations. *Cytokine.* 2001;14:27–36.
6. Rennen HJ, Boerman OC, Oyen WJ, van der Meer JW, Corstens FH. Specific and rapid scintigraphic detection of infection with ^{99m}Tc-labeled interleukin 8. *J Nucl Med.* 2001;42:117–123.
7. Rennen HJ, Boerman OC, Oyen WJ, Corstens FH. Kinetics of ^{99m}Tc-labeled interleukin 8 in experimental inflammation and infection. *J Nucl Med.* 2003; 44:1502–1509.
8. Gratz S, Rennen HJ, Boerman OC, Oyen WJ, Corstens FH. Rapid imaging of experimental colitis with ^{99m}Tc-interleukin 8 in rabbits. *J Nucl Med.* 2001;42: 917–923.

9. Gratz S, Rennen HJ, Boerman OC, Oyen WJ, Burma P, Corstens FH. 99mTc-Interleukin 8 for imaging acute osteomyelitis. *J Nucl Med.* 2001;42:1257–1264.

10. Rennen HJ, Bleeker-Rovers CP, van Eerd JE, et al. 99mTc-Labeled interleukin-8 for scintigraphic detection of pulmonary infections. *Chest.* 2004;126:1954–1961.

11. van der Laken CJ, Boerman OC, Oyen WJ, Van de Ven MT, Ven der Meer JW, Corstens FH. The kinetics of radiolabelled interleukin-8 in infection and sterile inflammation. *Nucl Med Commun.* 1998;19:271–281.

12. Laterveer L, Lindley IJ, Heemskerk DP, et al. Rapid mobilization of hematopoietic progenitor cells in rhesus monkeys by a single intravenous injection of interleukin-8. *Blood.* 1996;87:781–788.

13. Van Zee KJ, Fischer E, Hawes AS, et al. Effects of intravenous IL-8 administration in nonhuman primates. *J Immunol.* 1992;148:1746–1752.

14. Gross MD, Shapiro B, Fig LM, Steventon R, Skinner RW, Hay RV. Imaging of human infection with 131I-labeled recombinant human interleukin 8. *J Nucl Med.* 2001;42:1656–1659.

15. Abrams MJ, Juweid M, tenKate CI, et al. Technetium-99m-human polyclonal IgG radiolabeled via the hydrazino nicotinamide derivative for imaging focal sites of infection in rats. *J Nucl Med.* 1990;31:2022–2028.

16. Schwartz DA, Abrams MJ, Hauser MM, et al. Preparation of hydrazino-modified proteins and their use for the synthesis of 99mTc-protein conjugates. *Bioconjug Chem.* 1991;2:333–336.

17. Rennen HJ, van Eerd JE, Oyen WJ, Corstens FH, Edwards DS, Boerman OC. Effects of coligand variation on the in vivo characteristics of Tc-99m-labeled interleukin-8 in detection of infection. *Bioconjug Chem.* 2002;13:370–377.

18. Buijs WC, Massuger LF, Claessens RA, Kenemans P, Corstens FH. Dosimetric evaluation of immunoscintigraphy using indium-111-labeled monoclonal antibody fragments in patients with ovarian cancer. *J Nucl Med.* 1992;33:1113–1120.

19. Buijs WC, Siegel JA, Boerman OC, Corstens FH. Absolute organ activity estimated by five different methods of background correction. *J Nucl Med.* 1998;39:2167–2172.

20. International Commission on Radiological Protection. *Report of the Task Group on Reference Man.* Oxford, United Kingdom: Pergamon Press; 1975:89–91. ICRP Publication 23.

21. Stabin MG, Sparks RB, Crowe E. OLINDA/EXM: the second-generation personal computer software for internal dose assessment in nuclear medicine. *J Nucl Med.* 2005;46:1023–1027.

22. Palestro CJ, Kim CK, Swyer AJ, Vallabhajosula S, Goldsmith SJ. Radionuclide diagnosis of vertebral osteomyelitis: indium-111-leukocyte and technetium-99m-methylene diphosphonate bone scintigraphy. *J Nucl Med.* 1991;32:1861–1865.

23. van der Laken CJ, Boerman OC, Oyen WJ, van de Ven MT, van der Meer JW, Corstens FH. Radiolabeled interleukin 8: specific scintigraphic detection of infection within a few hours. *J Nucl Med.* 2000;41:463–469.